

KINETIC AND EQUILIBRIUM STUDY ON THE ADSORPTION OF METHYLENE BLUE FROM AQUEOUS SOLUTION ONTO COFFEE HUSK ACTIVATED CARBON

Le Van Khu¹, Ta Huu Son¹, Luong Thi Thu Thuy¹, Vu Thi Huong¹
Le Huu Dung¹ and Nguyen Dinh Hung²

¹*Faculty of Chemistry, Hanoi National University of Education*

²*Vinh Phuc Gifted High School*

Abstract. In this study, the adsorption kinetics and equilibrium of methylene blue from aqueous solution onto activated carbon derived from coffee husk using one step ZnCl₂ activation were investigated. The influence of initial methylene blue concentration and temperature were evaluated employing the batch experiment. To the experimental data, different kinetics and isotherm models were applied, finding that the best fitted is the pseudo-second-order equation and the Redlich-Peterson model, respectively. The mechanism of the adsorption was examined using the Weber and Morris model, and the obtained results suggested that the intra-particle diffusion was not the only rate-controlling step. The scale-up system was also designed for 50 - 90% methylene blue removal from an initial concentration of 100 mg L⁻¹ at 30 °C.

Keywords: activated carbon, methylene blue, adsorption kinetics, equilibrium of adsorption.

1. Introduction

Currently, water pollution with organic compounds is becoming an increasing concern issue by scientists and society. Dyes are used in many industries for dyeing, printing, painting, food coloring, and reported to cause eye burn, vomiting, cyanosis, jaundice, cancer, allergy, mutation, etc. Numerous techniques, including biological treatment, adsorption, filtration, coagulation, photodegradation, etc, are being developed. Among these methods, adsorption is a non-toxic, cost-effectiveness approach, especially at low adsorbate concentration or large scale applications [1]. Various adsorbents have been used for dye elimination from wastewater, such as perlite [2], orange peel [3], sugar beet pulp activated carbon [4], and kaolin [5]. Apart from general requirements for adsorbents, namely high mechanical and chemical stability, large specific surface area, a large number of functional groups, an effective adsorbent for dye

Received June 12, 2020. Revised June 23, 2020. Accepted June 29, 2020.

Contact Le Van Khu, e-mail address: khulv@hnue.edu.vn

removal should have a large number of mesopores that facilitating large dye molecules transport.

In this study, activated carbon (AC) from coffee husks using ZnCl_2 activation was used as adsorbent since it has a great number of mesopores, which is a proper adsorbent for dye molecules removal. Methylene blue (MB) is used as an adsorbate owing to the universal acceptance as a standard model of cationic dye. This study aims to evaluate the removal of MB from aqueous solution using coffee husk AC. Adsorption process was carried out by varying initial concentration of MB, contact time, and temperature to investigate the kinetics and equilibrium of the adsorption process.

2. Content

2.1. Experimental procedure

2.1.1. Adsorbent and adsorbate

Activated carbon developed from coffee husk by one step ZnCl_2 activation was used as adsorbent. The preparation of AC is summarized as following: Coffee husks (Arabica) were collected from a coffee mill in Son La Province of Vietnam. These were washed, dried, grounded, and finally sieved to fractions of 1.0 mm average particle size. The prepared coffee husk (CHF) was homogeneously mixed with ZnCl_2 (CAS: 7646-85-7, purity $\geq 98\%$, Xilong Chemical Co. Ltd, China, ZnCl_2/CHF mass ratio equal to 3) at $100\text{ }^\circ\text{C}$ for 1 h. It was heated at $100\text{ }^\circ\text{C}$ for 1 h and then oven-dried at $120\text{ }^\circ\text{C}$ for 12 h. The resulted samples were then activated under a nitrogen atmosphere (flow rate of 300 mL min^{-1}) at $600\text{ }^\circ\text{C}$ (heating rate of $10\text{ }^\circ\text{C min}^{-1}$) for 2 h. After cooling, the excess zinc chloride present in the carbonized material was leached out (for recycle) using dilute HCl solution. Then, the activated product was washed with hot distilled water until neutral pH and dried under vacuum at $120\text{ }^\circ\text{C}$ for 24 h. Finally, the activated carbon sample was grounded and sieved by mesh #100 and #50 to a particle size range of 0.15 - 0.3 mm. The specific surface area, mesopore surface area and pore volume of the sample, determined by BET method, are $1383\text{ m}^2\text{ g}^{-1}$, $922\text{ m}^2\text{ g}^{-1}$ and $1.6482\text{ cm}^3\text{ g}^{-1}$, respectively

The adsorbate, methylene blue (MB, CI = 52015; chemical formula: $\text{C}_{16}\text{H}_{18}\text{ClN}_3\text{S}$; molecular weight = 319.86 g mol^{-1} , a cationic dye supplied by Xilong Chemical Co. Ltd, China), was used without further purification. Double distilled water was used to prepare all of the solutions and reagents. MB concentration was determined at room temperature using a UV-Vis spectrophotometer (LIUV-310S) at 664.5 nm .

2.1.2. Methylene blue adsorption experiments

Kinetics experiments were conducted using 300 mL flasks containing 250 mL MB solution with different initial concentrations ($200 - 350\text{ mg L}^{-1}$) and 500 mg coffee husk AC samples. The mixtures were magnetic stirred at 200 rpm in a temperature-controlled water bath at a predetermined temperature ($10 - 40\text{ }^\circ\text{C}$). At a time-interval, about 5 mL of the mixtures were pipetted out, filtered, and analyzed for MB concentration.

The amount of MB adsorbed at time t , q_t (mg g^{-1}), and at equilibrium, q_e (mg g^{-1}), were calculated by

$$q_t = \frac{(C_o - C_t)V}{m} \tag{1}$$

$$q_e = \frac{(C_o - C_e)V}{m} \tag{2}$$

where C_o , C_t , and C_e (mg L^{-1}) are the MB concentrations at initial, any time t , and equilibrium, respectively. V is the volume of the solution (L), and m (g) is the mass of activated used.

Isotherm adsorption study of MB was carried out using batch experiments in 100 mL Erlenmeyer flasks. The mixtures of 100 mg AC sample and 50 mL MB solution with different initial concentrations (200 - 350 mg L^{-1}) were shaken at 120 rpm at four different temperatures of 10, 20, 30, and 40 °C for 18 h to reach equilibrium. The amount of MB adsorbed at equilibrium, q_e (mg g^{-1}), was calculated by using equation (2).

To ensure accuracy, each adsorption experiment was performed in triplicate, and the results are presented as mean values.

2.2. Results and discussion

2.2.1. Adsorption kinetics

* Effect of contact time, initial concentration, and temperature

For the kinetic adsorption of MB on coffee husk AC, the effect of initial concentration (200 - 350 mg L^{-1}), contact time (5 - 240 minutes), and temperature (10 - 40 °C) are illustrated in Figures 1a and 1b. The amount of MB adsorbed increased with an increase in contact time, speedily from 5 to 60 min, slowly from 60 to 150 min, and afterward approached the same values. Thus, the adsorption process is proved to reach the equilibrium stage after 240 min. The amount of MB adsorbed at time t and equilibrium increases with an increase in the initial MB concentration from 200 to 350 mg L^{-1} (Figure 1a). This might be ascribed to the increase in the driving force as a result of a higher concentration gradient [6].

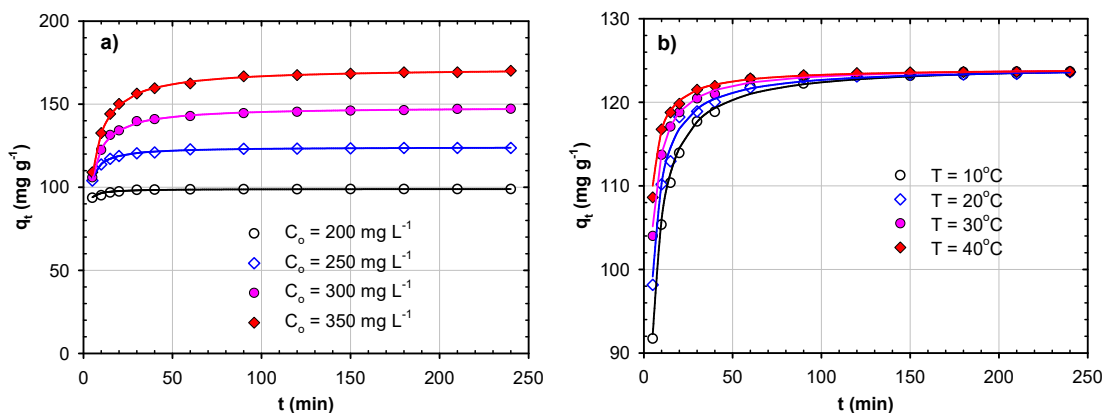


Figure 1. Adsorption kinetics of MB on the coffee husk activated carbon
(The solid curves were calculated by the PSO equation)

According to Figure 1b, the adsorption process is very fast at the initial stage up to 30 min then becomes slower in the range from 60 to 150 min. In this time, the adsorption rate is increased with an increase in temperature. However, after 150 min of contact time, the equilibrium was reached, and the MB adsorption capacity is the same, regardless of the temperature.

*** Kinetic model for the adsorption**

In order to investigate the adsorption of MB on coffee husk AC, three common kinetic models, namely the pseudo-first-order, pseudo-second-order, and Elovich, were evaluated to find the best fitted model for the experimental data. These models are expressed under linear form as follows:

Pseudo-first-order (PFO):

$$\ln(q_e - q_t) = \ln q_e - k_1 t \quad (3)$$

Pseudo-second-order (PSO):

$$\frac{t}{q_t} = \frac{1}{k_2 q_e^2} + \frac{1}{q_e} t \quad (4)$$

Elovich:

$$q_t = (1/\beta) \ln(\alpha\beta) + (1/\beta) \ln(t) \quad (5)$$

where q_t and q_e (mg g^{-1}) are the amounts of MB adsorbed at time t (min) and equilibrium; k_1 (min^{-1}) and k_2 ($\text{g mg}^{-1} \text{min}^{-1}$) are the PFO and PSO rate constants; α is initial adsorption rate ($\text{mg g}^{-1} \text{min}^{-1}$), and β is desorption constant (g mg^{-1}).

The suitability of the three models investigated is evaluated by the values of the coefficient of determination (R^2) and the average relative errors (ARE). The model with the highest R^2 value and the lowest ARE value is considered to be the most applicable model, which presents a good correlation between experimental data and kinetic equation, as well as between the experimental and predicted data. The value of R^2 and ARE were obtained by using equations (6) and (7).

$$R^2 = 1 - \frac{\sum_{i=1}^N (q_{t,\text{mes}} - q_{t,\text{pre}})_i^2}{\sum_{i=1}^N (q_{t,\text{mes}} - q_{t,\text{mean}})_i^2} \quad (6)$$

$$\text{ARE} = \frac{100}{N} \sum_{i=1}^N \left| \left(\frac{q_{t,\text{pre}} - q_{t,\text{mes}}}{q_{t,\text{mes}}} \right)_i \right| \quad (7)$$

where $q_{t,\text{mes}}$, $q_{t,\text{pre}}$ and $q_{t,\text{mean}}$ are experimental, predicted and the average amount of MB adsorbed at time t respectively; N is the number of experimental data.

Figure 2 illustrates the applying of PFO, PSO, and Elovich kinetic models for the adsorption of MB at an initial concentration of 200, 250, 300, and 350 mg L^{-1} , and the obtained kinetic parameters associated with the adsorption process are given in Table 1. It was observed that the experimental points are disorderly distributed along the PFO

and Elovich fitting lines, indicating a disagreement between the experimental data and that two models. In the case of PSO model, the linear lines go through almost all the experimental points, demonstrating its applicability in describing the MB adsorption process. Comparing the R^2 and ARE values of the three models in Table 1, R^2 values of the PSO model are close to unity and ARE values are very small ($\leq 0.40\%$). Besides, the q_e value of the PSO model is closer to the experimental q_e , indicating that MB adsorption on coffee husk AC follows the PSO kinetic model. The same results have reported for the adsorption of MB on AC from other precursors, such as date pits [7], pea shells [8], and sugar beet pulp [4].

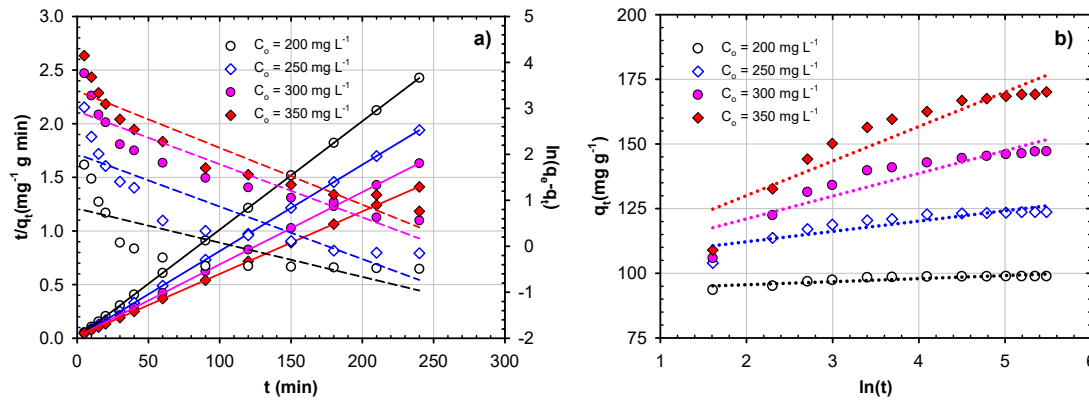


Figure 2. PFO and PSO kinetic models (a) and Elovich model (b) for MB adsorption at 30°C on the coffee husk AC

(The solid, dash, and dotted curves were calculated by the PSO, PFO, and Elovich equations)

It can be seen from Table 1 that the q_e obtained according to PSO model (as well as the experimental q_e values) increases with the increase of C_0 , while unchanged with the increase of temperature. q_e increases from 99.01 to 171.82 mg g^{-1} when C_0 varies from 200 to 350 mg g^{-1} , whereas slightly oscillate around 124.22 mg g^{-1} when temperature increase from 10 to 40 °C.

Given that the PSO model presented the best fit of the experimental data, the initial adsorption rate, h_0 ($\text{mg g}^{-1} \text{min}^{-1}$), at different initial MB concentrations and temperatures were calculated by the equation (8) and given in Table 1.

$$h_0 = k_2 q_e^2 \quad (8)$$

The initial adsorption rate decreases significantly from 374.5 to 57.0 $\text{mg g}^{-1} \text{min}^{-1}$ when C_0 increase from 200 to 350 mg L^{-1} , and slightly increase from 71.2 to 194.2 $\text{mg g}^{-1} \text{min}^{-1}$ when the temperature rises from 10 to 40 °C. The increase of h_0 with temperature is due to the increase in the diffusion rate of MB from the bulk solution to the AC surface, on the AC surface, as well as inside the pores at elevated temperature. Whereas the decrease of h_0 with C_0 can be explained by the higher probability of collision between dye molecules hence reduce the reaction between the dye and the active sites of the AC surfaces [9].

Table 1. Kinetic models calculated parameters in the MB adsorption on the coffee husk AC

C_0 (mg L ⁻¹)		200	250	300	350	250	250	250
T (°C)		30	30	30	30	10	20	40
Experimental q_e (mg g ⁻¹)		99.49	124.54	148.95	172.26	124.75	124.29	124.39
Pseudo first-order	q_e (mg g ⁻¹)	2.27	7.42	18.84	29.33	9.13	9.80	5.45
	$k_1 \times 10^2$ (min ⁻¹)	0.74	1.14	1.15	1.24	1.02	1.32	1.08
	R ²	0.5710	0.7686	0.8482	0.8667	0.8256	0.8105	0.7470
	ARE (%)	99.07	96.93	93.31	90.60	96.37	96.18	97.80
Pseudo second-order	q_e (mg g ⁻¹)	99.01	124.22	148.37	171.82	124.53	124.22	124.07
	$k_2 \times 10^3$ (g mg ⁻¹ min ⁻¹)	38.21	8.88	3.18	1.93	4.59	6.37	12.61
	h_0 (mg g ⁻¹ min ⁻¹)	374.5	137.0	70.0	57.0	71.2	98.2	194.2
	R ²	0.9999	0.9999	0.9999	0.9999	0.9999	0.9999	0.9999
	ARE (%)	0.26	0.19	0.39	0.40	0.34	0.38	0.19
Elovich	α (mg g ⁻¹ min ⁻¹)	2.94×10^{34}	8.59×10^{11}	1.14×10^6	3.07×10^4	3.17×10^6	5.75×10^8	2.42×10^{16}
	β (g mg ⁻¹)	0.850	0.250	0.114	0.075	0.145	0.189	0.336
	R ²	0.7711	0.7823	0.8323	0.8609	0.8312	0.7982	0.7643
	ARE (%)	0.69	1.72	2.95	3.67	2.71	2.18	1.33

*** Activation parameters**

The result in Table 1 shows that k_2 increase with the increasing of temperature, therefore, the PSO rate constant k_2 has been used to determine the activation energy E_a for MB adsorption onto coffee husk AC applying the Arrhenius equation:

$$\ln k_2 = \ln A - \frac{E_a}{RT} \quad (9)$$

where A is the Arrhenius factor, R is the gas constant (8.314 J mol⁻¹ K⁻¹), and T is the absolute temperature (K).

The plot of $\ln k_2$ versus reciprocal T (Figure 3) gives a straight line, and E_a was obtained from the slope of the linear plot and was estimated to be 24.759 kJ mol⁻¹. According to the literature [10], if E_a value is between 5 and 20 kJ mol⁻¹ physisorption is the predominant process, and if $E_a > 40$ kJ mol⁻¹, the chemical reaction process will take

place. Therefore, the adsorption of MB from aqueous solution onto coffee husk AC in this study is mainly physical and promoted by chemisorption.

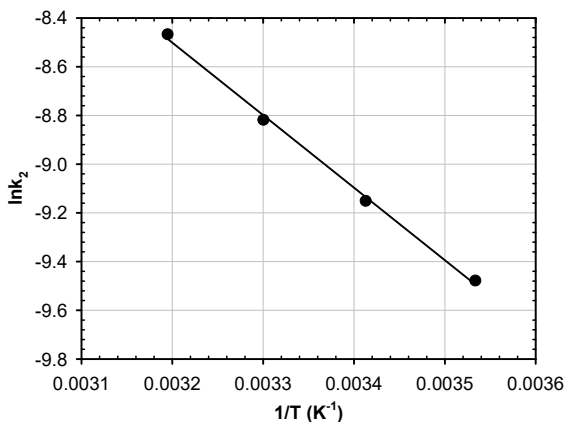


Figure 3. Plot of $\ln k_2$ vs $1/T$

*** Adsorption mechanism study**

The adsorption process is generally including three sequential processes: i) transport of the adsorbate to the external surface of the adsorbent (film diffusion), ii) transport of the adsorbate within the pores of the adsorbent and small amount of adsorption occur on the external surface (particle diffusion), and iii) physisorption or chemisorption of the adsorbate on the interior surface of the adsorbent [11]. Since the iii) process is generally accepted to be very fast compared to i) and ii) processes, the rate-limiting step may be either the film or the intra-particle diffusion or the combined effect of both diffusion ways. In order to establish the mechanism of the adsorption process and the rate controlling step, the intra-particle diffusion described by Weber and Morris [12] was used. This model is presented by the equation:

$$q_t = k_d t^{1/2} + C \tag{10}$$

where q_t (mg g⁻¹) is the amount of MB adsorbed at time t , k_d (mg g⁻¹ min^{0.5}) is the intra-particle diffusion rate constant, and C (mg g⁻¹) is a constant that reflects the thickness of the boundary layer effect.

The intra-particle diffusion model plot for MB adsorption on coffee husk AC is shown in Figure 4. In general, the linear of the plot q_t versus $t^{1/2}$ implicating that the intra-particle diffusion is included in the adsorption process. If the line passes through the origin, then the rate-controlling step is the intra-particle diffusion. If the plot does not pass through the origin, then apart from intra-particle diffusion, other kinetic steps are involved in the adsorption process [13]. As illustrated in Figure 4, for all experimental conditions investigated, the plots q_t versus $t^{1/2}$ are made up of three separate linear steps: i) at the beginning of adsorption, the sharp increase of linear representing the rapid surface loading due to the strong attraction between MB and the outer surface of coffee husk AC; ii) in the second stage (25 - 90 min), the lines are less steep with smaller slope, which illustrate a lower adsorption rate per unit time. This is

the gradual adsorption step, and intra-particle diffusion of MB within the pores of AC is the rate limiting. The value of the intercept C of the plots is proportional to the thickness of the layer on the AC surface that hinders the diffusion of MB, and iii) after 90 min, the lines are parallel to the horizontal axis, illustrating the final equilibrium when the adsorption and desorption rates of MB are equal. Similar behavior was reported for the adsorption of MB onto modified Tamazert kaolin [5], papaya seeds [14], born char [15].

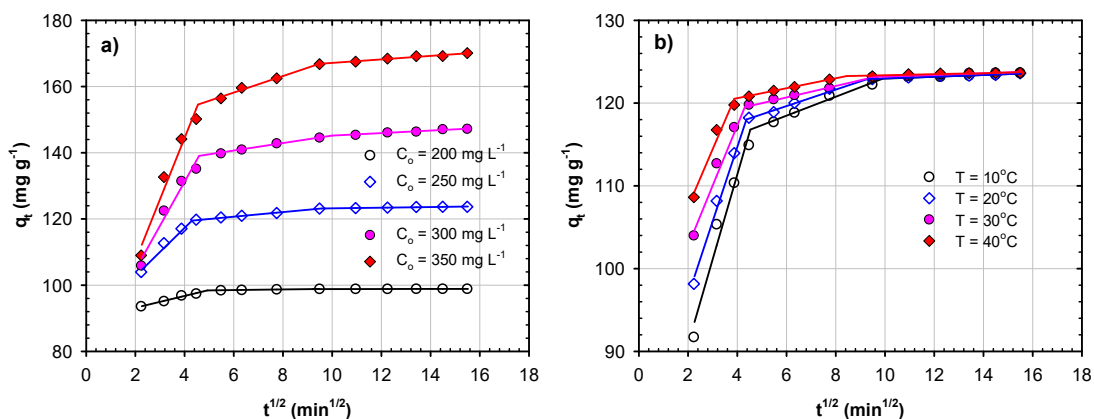


Figure 4. Intraparticle diffusion model plot for MB adsorption on coffee husk AC
(a) with different initial concentrations at $T = 30\text{ }^{\circ}\text{C}$
(b) at different temperatures with $C_o = 250\text{ mg L}^{-1}$

Table 2. Calculated parameters of the Weber and Morris model for MB adsorption on coffee husk AC

C_o (mg L^{-1})	T ($^{\circ}\text{C}$)	k_{d1} ($\text{mg g}^{-1} \text{min}^{-0.5}$)	C_1 (mg g^{-1})	R_1^2	k_{d2} ($\text{mg g}^{-1} \text{min}^{-0.5}$)	C_2 (mg g^{-1})	R_2^2
200	30	1.78	89.63	0.9830	0.09	97.96	0.9819
250	30	7.26	88.23	0.9897	0.69	116.53	0.9946
300	30	13.28	78.10	0.9637	1.13	133.86	0.9930
350	30	18.55	70.27	0.9649	2.49	143.23	0.9898
250	10	10.24	70.40	0.9643	1.15	111.60	0.9794
250	20	8.98	78.78	0.9905	0.99	113.67	0.9764
250	40	6.92	93.68	0.9669	0.60	118.18	0.9984

The calculated parameters of intra-particle diffusion model for the two first steps are listed in Table 2. It can be observed from Table 2 that the value of k_{d1} was higher than that of k_{d2} , indicating the rate of adsorption is initially slightly faster and then slows down and this could be attributed to the limitation of the available vacant sites for

diffusion in and pore blockage by the adsorbed MB molecules on the AC surface. The obtained results suggest that the process of MB adsorption on coffee husk AC was controlled by external mass transfer followed by intraparticle diffusion mass transfer.

2.2.2. Equilibrium of adsorption

The experimental results of the relationship between q_e and C_e at four temperatures from 10 to 40 °C and the research on the effect of temperature in the kinetic section show that, with the same C_e , the q_e value is independent of temperature. This concludes that adsorption temperature has only a significant effect on the adsorption rate while having an unclear effect on equilibrium adsorption. Therefore, this section only introduces and discusses on experimental adsorption equilibrium data obtained at 30 °C.

To understand the interaction between adsorbate and adsorbent, the amount of adsorbate uptake and the adsorbate concentration remaining in solution was modeled, using different isotherm models. The two adsorption isotherm models with two-parameters, including Langmuir and Freundlich, and three adsorption isotherm models with three-parameters, including Redlich-Peterson, Sips, and Toth, are in their non-linear forms and shown in Table 3.

Table 3. Isotherm models and the parameters involved

Isotherm	Expression	Parameters	Ref.
Langmuir	$q_e = \frac{q_m K_L C_e}{1 + K_L C_e}$	q_m : maximum monolayer coverage capacity K_L : Langmuir isotherm constant	[16, 17]
Freundlich	$q_e = K_F C_e^{1/n}$	K_F : Freundlich isotherm constant n : parameter related to multiple layer coverage	[18]
Redlich–Peterson	$q_e = \frac{A C_e}{1 + B C_e^\beta}$	A, B : Redlich–Peterson isotherm constant β : Redlich–Peterson model exponent	[19]
Sips	$q_e = \frac{q_{m_s} K_S C_e^{m_s}}{1 + K_S C_e^{m_s}}$	q_{m_s} : Sips maximum adsorption capacity K_S : Sips equilibrium constant m_s : Sips model exponent.	[19]
Tóth	$q_e = \frac{q_{m_T} C_e}{(1 / K_T + C_e^{m_T})^{1/m_T}}$	q_{m_T} : Toth maximum adsorption capacity K_T : Toth equilibrium constant m_T : Toth model exponent	[19]

The parameters of the five isotherms equations for the MB adsorption on coffee husk AC were evaluated using non-linear regression by minimizing the root mean square error (RMSE). The applicability of these equations is verified through the

coefficient of determination (R^2) and the average relative errors (ARE). RMSE, R^2 and ARE are calculated according to equations (11), (12), and (13), respectively.

$$\text{RMSE} = \sqrt{\frac{1}{N} \sum_{i=1}^N (q_{e,\text{pre}} - q_{e,\text{mes}})_i^2} \quad (11)$$

$$R^2 = 1 - \frac{\sum_{i=1}^N (q_{e,\text{mes}} - q_{e,\text{pre}})_i^2}{\sum_{i=1}^N (q_{e,\text{mes}} - q_{e,\text{mean}})_i^2} \quad (12)$$

$$\text{ARE} = \frac{100}{N} \sum_{i=1}^N \left| \left(\frac{q_{e,\text{pre}} - q_{e,\text{mes}}}{q_{e,\text{mes}}} \right)_i \right| \quad (13)$$

where $q_{e,\text{mes}}$, $q_{e,\text{pre}}$ and $q_{e,\text{mean}}$ are the experimental, predicted, and average adsorption capacities, respectively; N is the number of experimental data.

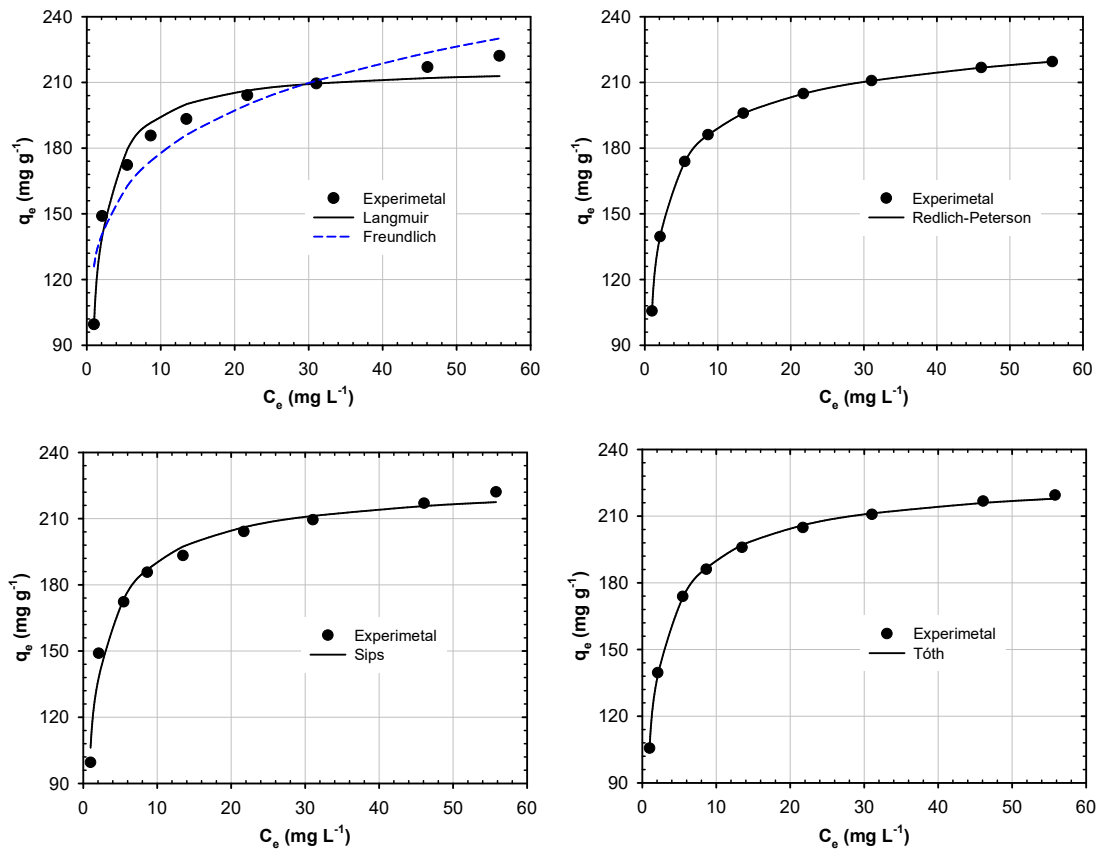


Figure 5. Comparison of the experimental and the predicted adsorption isotherms of MB onto coffee husk AC at 30 °C according to Langmuir, Freundlich, Redlich-Peterson, Sips, and Toth equations

Figure 5 illustrates the experimental adsorption isotherms (the black dots) and the two-parameter and three-parameter isotherm models that are fitted to the experimental data obtained at 30 °C. It can be seen that the experimental data are well described by Redlich-Peterson, Toth, and Sips models since the experiment points are all lied on the calculated isotherm lines. The parameters of the five used isotherm models are presented in Table 4. It can be seen that the R^2 values of three-parameters isotherms are closer to unity than that of two-parameters isotherms. Furthermore, RMSE and ARE values of three-parameters isotherms are relatively lower. This suggesting that the three-parameters isotherms provide a better fit than the two-parameters isotherms. Among the three-parameters models, Redlich-Peterson presents the best fit of all, since R^2 is closest to unity, RMSE, and ARE values are smallest, suggesting that the adsorption process is a mix and does not follow ideal monolayer adsorption [20]. Nevertheless, Sips and Toth models also can describe the investigated adsorption process quite well, considering that the R^2 and ARE values are acceptable ($R^2 > 0.98$ and $ARE < 2.5\%$).

Table 4. Parameters of the Langmuir, Freundlich, Redlich-Peterson, Sips, and Toth isotherms for the adsorption of MB onto coffee husk AC at 30 °C

Model	Parameters		RMSE	R^2	ARE (%)
Langmuir	q_m (mg g ⁻¹)	217.32	6.05	0.9729	2.79
	K_L (L mg ⁻¹)	0.861			
Freundlich	K_F (mg ^{1-1/n} L ^{1/n} g ⁻¹)	126.06	11.40	0.9040	6.33
	n	6.684			
Redlich–Peterson	A (L g ⁻¹)	252.00	4.00	0.9882	1.91
	B (L mg ⁻¹) ^β	1.378			
	β	0.951			
Sips	q_{m_s} (mg g ⁻¹)	229.86	4.87	0.9825	2.45
	K_s (L mg ⁻¹) ^{m_s}	0.863			
	m_s	0.749			
Toth	q_{m_T} (mg g ⁻¹)	232.43	4.69	0.9837	2.35
	K_T (L mg ⁻¹) ^{m_T}	1.418			
	m_T	0.683			

The q_m value calculated by the Toth equation is 232.43 mg g⁻¹, suggesting that the coffee husk AC has a good adsorption capacity for MB adsorption, and is comparable with kaolin (111 mg g⁻¹) [5], silica gel supported calix[4]arene cage (212.770 mg g⁻¹) [21], and industrial softwood waste Cedar (217.39 mg g⁻¹) [22].

2.2.3. Scale-up design

The amount of coffee husk AC required to achieve the pre-determined removal efficiency was estimated by applying data from the best fitted adsorption isotherm

$$W = \frac{V(C_o - C_t)}{q_t} = \frac{V(C_o - C_e)}{q_e} \quad (14)$$

where V is the volume; C_o , C_t , and C_e are the MB concentration at initial, any time t , and equilibrium; q_t , q_e are the amount of MB adsorbed at any time t and equilibrium; W (g) is the mass of the AC needed. q_e is calculated from the parameters in Table 4 using the best fitted Redlich–Peterson equation, the equation (14) is modified as equation (15)

$$W = \frac{V(C_o - C_e)(1 + 1.378C_e^{0.951})}{252.00C_e} \quad (15)$$

Table 5 presents the calculated coffee husk AC amount needed in order to achieve MB removal from 50 to 90% with an initial MB concentration of 100 mg L⁻¹ and MB solution volume from 2 to 10 L.

Table 5. Weight of activated carbon (g) for the removal of MB (%) at 30 °C for different volumes of MB solution

V (L)	50%	60%	70%	80%	90%
2	0.459	0.560	0.667	0.787	0.951
4	0.919	1.119	1.333	1.574	1.901
6	1.378	1.679	2.000	2.362	2.852
8	1.838	2.238	2.666	3.149	3.803
10	2.297	2.798	3.333	3.936	4.753

It can be seen from Table 6 that the weight of coffee husk AC needed for the removal of MB is relatively low. The required amount of AC to remove 50 and 90% of the initial MB concentration are 0.2297 and 0.4753 g L⁻¹, respectively. This result suggests the effectiveness of coffee husk AC on the removal of MB from wastewater.

3. Conclusions

In this work, the adsorption properties of MB onto coffee husk activated carbon was investigated using a batch experiment with different MB initial concentrations of 200 - 350 mg L⁻¹ and a range of the temperatures from 10 to 40 °C. The kinetic studies showed that the adsorption process is fast and followed pseudo-second-order equation, with the activation energy (E_a) is 24.759 kJ mol⁻¹. The adsorption process was controlled by external mass transfer followed by intraparticle diffusion mass transfer. The equilibrium data is fitted well with the Redlich-Peterson model, from which, the scale-up system was designed up to 10 L MB solution (100 mg L⁻¹) at 30 °C for 50 to 90% MB removal. The experimental data obtained in the present study indicated that activated carbon developed from coffee husk by ZnCl₂ activation follow one-step

process is a suitable candidate for use as adsorbents in the removal of cationic dyes in wastewater.

REFERENCES

- [1] L.G.C. Villegas, N. Mashhadi, M. Chen, D. Mukherjee, K.E. Taylor, N. Biswas, 2016. A Short Review of Techniques for Phenol Removal from Wastewater. *Curr. Pollut. Rep.*, Vol. 2, pp. 157-167.
- [2] M. Dogan, M. Alkan, Y. Onganer, 2000. Adsorption of methylene blue from aqueous solution onto perlite. *Water, Air, and Soil Pollution*, Vol. 120, pp. 229-248.
- [3] P.S. Kumar, P.S.A. Fernando, R.T. Ahmed, R. Srinath, M. Priyadharshini, A.M. Vignesh, A. Thanjiappan, 2014. Effect of temperature on the adsorption of methylene blue dye onto sulfuric acid-treated orange peel. *Chem. Eng. Comm.*, Vol. 201, pp. 1526-1547.
- [4] D. Li, J. Yan, Z. Liu, Z. Liu, 2016. Adsorption kinetic studies for removal of methylene blue using activated carbon prepared from sugar beet pulp. *Int. J. Environ. Sci. Technol.*, Vol. 13, pp. 1815-1822.
- [5] A. Boukhemkhem, K. Rida, 2017. Improvement adsorption capacity of methylene blue onto modified Tamazert kaolin. *Adsorpt. Sci. Technol.*, Vol. 35, Iss. 9-10, pp. 753-773.
- [6] Y.J. Yao, H. Bing, F. Xu, F. Chen, 2011. Equilibrium and kinetic studies of methyl orange adsorption on multiwalled carbon nanotubes. *Chem. Eng. J.*, Vol. 170, Iss. 1, pp. 82-89.
- [7] S.S. Ashour, 2010. Kinetic and equilibrium adsorption of methylene blue and remazol dyes onto steam-activated carbons developed from date pits. *Journal of Saudi Chemical Society*, Vol. 14, pp. 47-53.
- [8] U. Gecgel, G. Ozcan, G.C. Gurpinar, 2013. Removal of Methylene Blue from Aqueous Solution by Activated Carbon Prepared from Pea Shells (*Pisum sativum*). *Journal of Chemistry*, Vol. 2013, Article ID 614083.
- [9] K.K. Wong, C.K. Lee, K.S. Low, M.J. Haron, 2003. Removal of Cu and Pb by tartaric acid modified rice husk from aqueous solutions. *Chemosphere*, Vol. 50, pp. 23-28.
- [10] T.S. Anirudhan, P.G. Radhakrishnan, 2008. Thermodynamics and kinetics of adsorption of Cu(II) from aqueous solutions onto a new cation exchanger derived from tamarind fruit shell. *J. Chem. Thermodynamics*, Vol. 40, pp. 702-709.
- [11] S. Karthikeyan, B. Sivakumar, N. Sivakumar, 2010. Film and Pore Diffusion Modeling for Adsorption of Reactive Red 2 from Aqueous Solution on to Activated Carbon Prepared from Bio-Diesel Industrial Waste. *J. Chem.*, Vol. 7, Article ID 138684.
- [12] Y.S. Ho, J.C.Y. Ng, G. McKay, 2000. Kinetics of pollutant sorption by biosorbents: Review. *Sep. Purif. Technol.*, Vol. 29, Iss. 2, pp. 189-232.
- [13] A. Radjenovic, G. Medunje, 2020. Dynamics and thermodynamics of a nickel uptake from a water system onto the blast furnace sludge. *Journal of Chemical Technology and Metallurgy*, Vol. 55, pp. 110-118.

- [14] B.H. Hameed, 2009. Evaluation of papaya seeds as a novel non-conventional low-cost adsorbent for removal of methylene blue. *J. Hazard. Mater.*, Vol. 162, pp. 939-944.
- [15] P. Jia, H. Tan, K. Liu, W. Gao, 2018. Removal of methylene blue from aqueous solution by bone char. *Appl. Sci.*, Vol. 8, Article ID 1903.
- [16] A.M. Brown, 2001. A step-by-step guide to non-linear regression analysis of experimental data using a Microsoft Excel spreadsheet. *Comput. Meth. Prog. Bio.*, Vol. 65, pp. 191-200.
- [17] O. Hamdaoui, E. Naffrechoux, 2007. Modeling of adsorption isotherms of phenol and chlorophenols onto granular activated carbon: Part I. Two-parameter models and equations allowing determination of thermodynamic parameters. *J. Hazard. Mater.*, Vol. 147, pp. 381-394.
- [18] K. Le Van, D.M. Truong, 2015. Adsorption of methylene blue from aqueous solution using activated carbon derived from coffee husks. *Journal of Science of HNUE, Chemical and Biological Sci.*, Vol. 60, pp. 32-43.
- [19] N. Ayawei, A.N. Ebelegi, D. Wankasi, 2017. Modelling and Interpretation of Adsorption Isotherms. *J. Chem.*, Vol. 2017, Article ID 3039817.
- [20] F. Brouers, T. J. Al-Musawi, 2015. On the optimal use of isotherm models for the characterization of biosorption of lead onto algae. *Journal of Molecular Liquids*, Vol. 212, pp. 46-51.
- [21] F. Temel, M. Turkyilmaz, S. Kucukcongar, 2020. Removal of methylene blue from aqueous solutions by silica gel supported calix[4]arene cage: Investigation of adsorption properties. *Eur. Polym. J.*, Vol. 125, Article ID 109540.
- [22] M.E. Hajam, N.I. Kandri, A. Harrach, A.E. Khomsi, A. Zerouale, 2019. Adsorption of Methylene Blue on industrial softwood waste “Cedar” and hardwood waste “Mahogany”: a comparative study, *Materialstoday: Proceedings*, Vol. 13, pp. 812-821.